Applied Catalysis B: Environmental 132–133 (2013) 212–218

Contents lists available at SciVerse ScienceDirect

Applied Catalysis B: Environmental

journal homepage: www.elsevier.com/locate/apcatb

Effect of water vapor on the by-products and decomposition rate of ppb-level toluene by photocatalytic oxidation

Jinhan Mo, Yinping Zhang*, Qiujian Xu

Department of Building Science, Tsinghua University, Beijing 100084, PR China

ARTICLE INFO

Article history:
Received 14 September 2012
Received in revised form
26 November 2012
Accepted 2 December 2012
Available online 10 December 2012

Keywords:
Photocatalytic oxidation (PCO)
Volatile organic compounds (VOCs)
Indoor air quality (IAQ)
Air cleaning

ABSTRACT

It was found that there were unwanted by-products in the photocatalytic oxidation (PCO) of indoor ppb-level toluene, a typical volatile organic compound (VOC) in indoor air. However, up to now the control mechanism of the generation of the products has not been clear. In this study we address the problem: a titania-coated glass-plate reactor was applied to study the by-products and decomposition rate; the by-products generated under a series of water vapor concentrations were instantaneously identified by proton transfer reaction-mass spectrometer (PTR-MS); the results indicate that water vapor has a significant effect not only on the photocatalytic decomposition rate of toluene, but also on its by-products generation; the competitive adsorption mechanism between water vapor, toluene and its by-products was analyzed. By-products may make the typical Langmuir–Hinshelwood model unfeasible in real application. A health risk assessment of the by-products was also introduced. The results show that the maximum decomposition efficiency does not always lead to minimal by-products and lowest health risk. What it does show is that when evaluating the performance of photocatalytic air purification, health risks posed by the by-products should be the primary concern rather than the decomposition efficiency.

1. Introduction

In modern indoor environments, many materials and products emit harmful contaminants, such as toluene, benzene and formaldehyde [1–4]. These contaminants influence human health, comfort and productivity [5]. Some have been found to be associated with asthma, nasopharyngeal cancer and multiple subjective health complaints [6]. Photocatalytic oxidation (PCO) is an innovative approach to eliminating volatile organic compounds (VOCs) indoors [7,8] and has been investigated by many researchers [9–11]. The results of complete PCO for VOCs should be CO_2 and H_2O. Such a reaction seems perfect for removing VOCs from the air since both CO_2 and H_2O are nontoxic. Indoor air cleaners based on the PCO approach have been developed and are commercially available. However, recent studies [12–15] have found that the photocatalytic reactions are not as complete as they are assumed to be. The photocatalytic oxidation process sometimes stops along the way, yielding aldehydes, ketones or organic acids [16]. Some of these unwanted by-products are relatively more harmful to people's health than the original contaminants [13].

Logically, the by-product generation is influenced by the photocatalytic degradation route, which is controlled through the reaction conditions (the irradiation intensity of ultraviolet light, concentrations of pollutants and humidity, reaction temperature etc.) [17]. In previous studies, the water vapor level was found to play an extremely important role in photocatalytic oxidation. The adsorbed water molecules on the reaction surface are the main source of hydroxyl radicals $OH^{\bullet}$, which is the dominant strong oxidant for pollutant decomposition. It has been reported that under UV illumination, the number of hydroxyl radicals formed is directly proportional to the adsorbed water molecules [18]. However, excessive water vapor on the catalyst surface will inhibit the reaction rate because the presence of water vapor competes with pollutants for adsorption sites on the photocatalyst, thus reducing the pollutant removal rate [19–21]. Normally, the influence of water vapor on PCO reactions follows the adsorption competition relationship. With an increase of water vapor, the PCO reaction rate will initially increase before decreasing, with a maximum value in between [20].

However, there are few studies relating to the effect of water vapor on the generation of PCO by-products [15,22,23]. In this work we studied the effect of water vapor (typical indoor levels, relative humidity: 0–70%) on the PCO by-products and decomposition rate of ppb-level toluene.

2. Experimental

2.1. UV-PCO reaction setup

The experiment was carried out in a stainless steel plate-type UV-PCO reactor [13]. Two photocatalyst-coated glass plates

* Corresponding author. Tel.: +86 10 6277 2518; fax: +86 10 6277 3461.
E-mail address: zhangyp@tsinghua.edu.cn (Y. Zhang).

0926-3373/$ – see front matter © 2012 Elsevier B.V. All rights reserved.
http://dx.doi.org/10.1016/j.apcatb.2012.12.001

(76.0 mm × 25.0 mm × 1.0 mm) were placed in the reactor. The photocatalyst powders (commercial Degussa P25, with a primary particle diameter of 300 nm, a specific surface area of 50 m^2/g, and a crystal distribution of 70% anatase and 30% rutile) were deposited on the glass plate as a film using the dip-coating method [13] with a net weight of 22 mg loading on the reaction side. Compressed air from a gas cylinder was divided into two streams. One stream passed through a mass flow controller and the other passed through a bottle-wash humidifier to control the humidity. The gas from another cylinder with 500 ppmv toluene was mixed with the compressed air and then was supplied to the plate-type PCO reactor. All the air-flow rates were controlled by two mass flow controllers. Two UV-C lamps (Philips Hg-Lamp, TUV 15W G15T8 UV-C, made in Holland) with a peak UV radiation at 254 nm were used to irradiate the reactor through a quartz glass.

2.2. PTR-MS measurement

A standard type of PTR-MS (*P*roton *T*ransfer *R*eaction-*M*ass *S*pectrometer, Ionicon Analytik, Austria) was applied to detect the gas-phase concentrations of various pollutants at sub-ppbv levels [13,16,24]. The *M*ass-*I*dentification-*D*etection (MID) mode of the PTR-MS was used during the research. MID was used to continuously trace some specific compounds identified from the mass-scan mode [13]. The temperatures of the detection chamber and the sampling tube were set to 60 °C. Toluene (m/z 93 signal) measured by the PTR-MS was calibrated by the gas chromatography–mass spectrometry method and its measurement accuracy was ±10%. For formaldehyde (m/z 31 signal), it was calibrated by the MBTH (3-methyl-2-benzothiazolinonehydrazone hydrochloride) spectrophotometry method under various water vapor levels and its measurement accuracy was ±5%. For other organic by-products, the measurement accuracy of the PTR-MS was estimated at ±25%.

2.3. Experimental conditions

All the experiments were performed at a common indoor air conditioning level with a temperature of 25.0 ± 1.0 °C, and a *r*elative *h*umidity (RH) of 3–70%. Inlet concentrations of toluene were adjusted in the range of 90–800 ppbv. The total airflow rate through the PCO reactor was kept at 0.55 l/min with a residence time of 0.2 s. The UV radiation intensity on the reaction surface was 0.43 mW/cm^2 at the wavelength of 254 nm which was measured using a UV-C power meter (HANDY 176, made in China). Firstly, the air-flow rate and inlet concentration of toluene were set. After the reactor inlet/outlet toluene concentration reached steady state, water vapor with high concentration was introduced from the inlet of reactor. When the inlet/outlet toluene and water vapor concentrations reached a steady state, the UV lamp was turned on to illuminate the reaction surface. All reported measurements were taken after the effluent pollutants concentration reached a sustained level. Secondly, an adjustment was made to reduce the inlet water vapor concentration. When the inlet toluene and water vapor reached a new steady state, the UV lamp was turned on and a new set of measurements taken. These adjustments were made 5–8 times under various inlet toluene concentrations (90–800 ppbv). All experiments at each inlet toluene concentration were repeated twice and 3 times for 400 and 800 ppbv. After each experiment, the TiO_2 films were photochemically regenerated by continuous illumination (94 mW/cm^2) and flow of humid air (RH = 60%) through the reactor overnight, in order to remove the possible, strongly adsorbed by-products.

2.4. Data analysis

The photocatalytic oxidation efficiency of toluene, ε was defined as

$$\varepsilon = \frac{C_{\text{inlet}} - C_{\text{outlet}}}{C_{\text{inlet}}} \quad (1)$$

where C_{inlet} and C_{outlet} are the inlet and outlet toluene concentrations, respectively.

The average reaction flux was obtained from the mass balance in the reactor:

$$r = \frac{G(C_{\text{inlet}} - C_{\text{outlet}})}{A} = \frac{GC_{\text{inlet}}\varepsilon}{A} \quad (2)$$

where r is the average reaction flux per surface area, G is the gas flow rate and A is the total surface area (specific surface area times the total amount of P25). In this study, A is equal to 2.2 m^2 for the photocatalyst-coated reaction films.

The carbon balance was analyzed through summing the concentration of carbon atoms from all detected compounds. The carbon balance ratio between outlet and inlet, η_{carbon}, was defined as

$$\eta_{\text{carbon}} = \frac{\sum_i C_{\text{outlet},i} \times (\text{number of carbon atoms of compound } i)}{\sum_j C_{\text{inlet},j} \times (\text{number of carbon atoms of compound } j)} \quad (3)$$

The risk assessment to human health of these by-products was introduced through a health-related index (HRI) [13]. It was:

$$\text{HRI}_i = \frac{C_i}{\text{REL}_i} \quad (4)$$

where REL_i is the recommended exposure limit of compound i. Some research institutes have published the REL values of various VOCs (Table 1), such as U.S. NIOSH (National Institute for Occupational Safety and Health). If HRIi exceeds the value 1, it indicates that the concentration of compound i is larger than its REL, that is, it will cause health risk to human being. HRI is used to quantify the effect of harmful by-products below. The HRI values of any carcinogenic compounds were summed to present the carcinogenic risk of PCO by-products:

$$\text{HRI}_{\text{car}} = \sum_i \text{HRI}_{\text{car},i} \quad (5)$$

3. Results

3.1. Effect of water vapor on the decomposition rate of toluene

Formaldehyde, methanol, propylene, acetaldehyde, benzaldehyde, etc. were found to be the main photocatalytic by-products of toluene in our previous research [13]. In the present study, the concentration changes of these compounds during the photocatalyic reaction were traced through the PTR-MS. Fig. 1 shows the changes of toluene and its main by-products versus the relative humidity, with an inlet toluene concentration of 400 ppbv. It was seen that the outlet toluene concentrations decreased when the water vapor levels were reduced from 62.1 to 16.0% (Fig. 1(a)). This indicated that the lower water vapor levels promoted the photocatalytic oxidation of toluene. However, when the water vapor level was 3.1%, the outlet concentration of toluene increased gradually until it finally almost reached the inlet concentration of toluene (Fig. 1(b)). This demonstrated that the TiO_2 film was being deactivated during the photocatlytic reaction.

Fig. 2 summarizes the photocatalytic oxidation efficiencies of toluene versus water vapor levels with the inlet toluene concentrations of 90, 145, 250, 400, 600, 700 and 800 ppbv. It shows that the profiles of toluene oxidation efficiency varied significantly with water vapor concentrations. When the inlet toluene concentrations were lower than 250 ppbv, the efficiencies always decreased

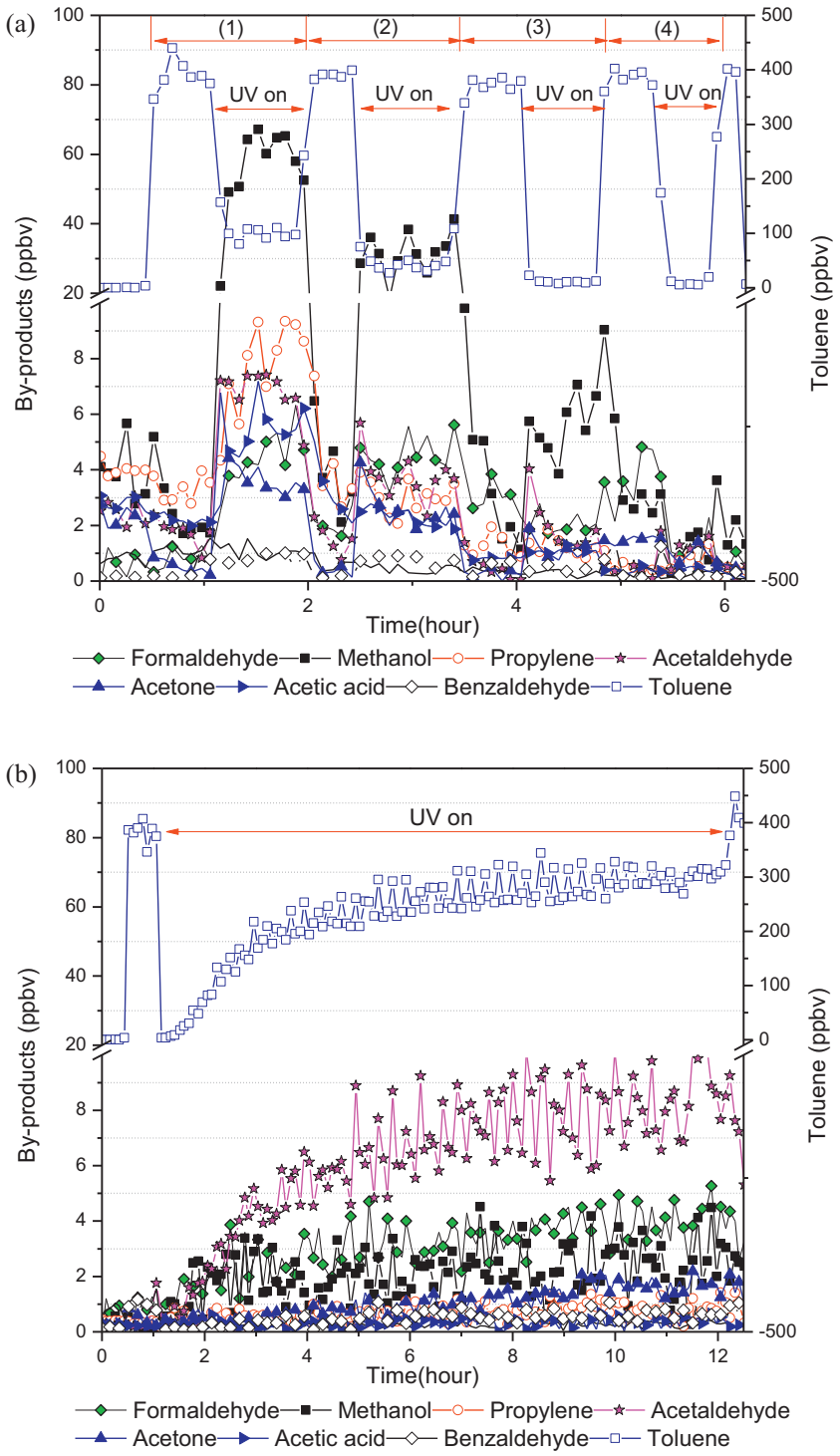

Fig. 1. Toluene and its main by-products conversions versus time with inlet toluene concentration of 400 ppbv, $T = 25.0 \pm 1.0\,^{\circ}C$ and UV intensity = 0.43 mW/cm^2. (a): (1) inlet humidity level is 62.1%; (2) 44.8%; (3) 27.2%; (4) 16%. (b): inlet humidity level is 3.1%.

with increasing humidity. When the inlet toluene concentrations were higher than 250 ppbv, the oxidation efficiency increased first and then dropped down with the increasing of water vapor levels. A maximum efficiency was obtained at an optimal humidity (see Fig. 2). Obee and Hay [20] got a similar result when studying the photo-oxidation of ethylene on TiO_2. In addition, when the inlet toluene concentrations were higher than 700 ppbv and the water vapor levels were lower than about 5%, the toluene oxidation efficiencies trended to zero indicating that significant deactivations were occurring under such conditions, similar to what is shown in Fig. 1(b).

3.2. *Effect of water vapor on the gas-phase by-products of toluene*

Water vapor also has a strong influence on the gas-phase by-products generation of toluene. At high water vapor concentrations, the gas-phase by-products consisted mainly of low molecular weight compounds, such as methanol, acetaldehyde and

Table 1
Recommended exposure limit (REL) values of some compounds.

Pollutants	IARC carcinogenic classification[a]	REL (ppmv)	REL data sources
Acetaldehyde	Group 2B, possibly carcinogenic to humans	0.078	*Office of Environmental Health Hazards Assessments, California Environmental Protection Agency, U.S.* (*OEHHA*)
Benzene	Group 1, carcinogenic to humans	0.019	
Formaldehyde	Group 1, carcinogenic to humans	0.007	
Methanol	–	4	
Toluene	Group 3, not classifiable as to its carcinogenicity to humans	0.080	
Acetone	–	250	*The National Institute for Occupational Safety and Health, U.S.* (*NIOSH*)
Acetic acid	–	10	
Benzaldehyde	–	2	*American Industrial Hygiene Association* (*AIHA*) *recommends a Workplace Environmental Exposure Level* (*WEEL*)

[a] Agents classified by the IARC (International Agency for Research on Cancer Agents) Monographs, volumes 1–104, 2012.

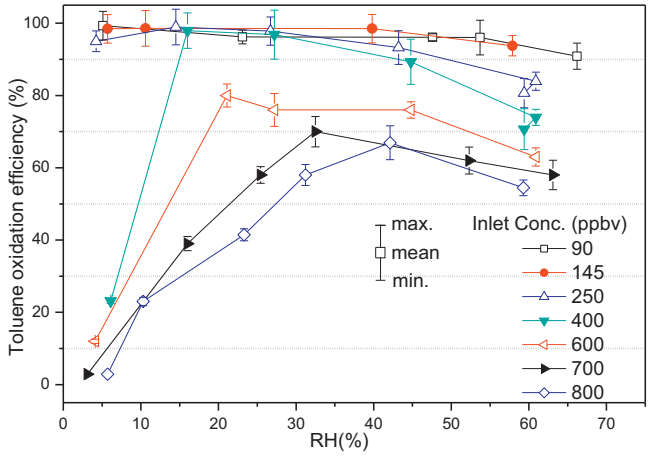

Fig. 2. Toluene oxidation efficiency versus relative humidity at inlet toluene concentrations of 90–800 ppbv.

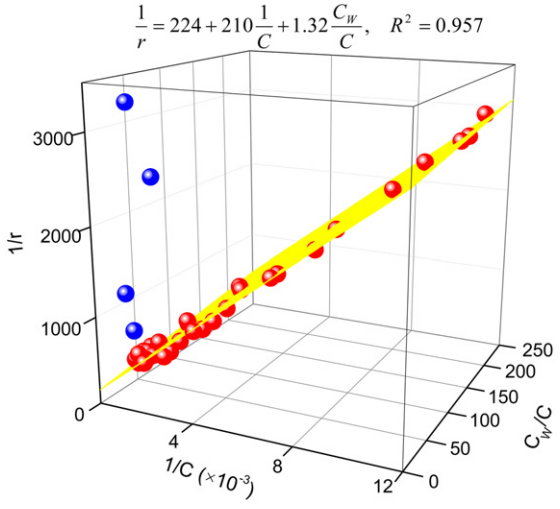

Fig. 3. Plot according to Eq. (8) with inlet toluene concentrations of 90–800 ppbv, water vapor concentrations of 900–21,000 ppmv and UV intensity of 0.43 mW/cm^2. The red dots are the data used for the fitting. The blue dots are the outliers with low relative humidity. The yellow plane is the 3D surface with the equation shown on the top. All data was shown in Table S1 in the Supporting Information. (For interpretation of the references to color in this figure legend, the reader is referred to the web version of the article.)

propylene (Fig. 1(a)), but there were also some high molecular weight by-products, benzaldehyde etc. With the decline of relative humidity levels from 62.1 to 16.0%, fewer gas-phase by-products were detected and the decomposition rate of toluene was increasing, up to 98% when relative humidity was 16.0%. When the water vapor level was 3.1% (Fig. 1(b)), a significant decrease in the toluene decomposition rate was observed over the reaction time. Acetaldehyde, formaldehyde and methanol were the main gas-phase by-products in this case.

The International Agency for Research on Cancer (IARC) has classified the carcinogenic risk to humans of some by-products, such as formaldehyde, acetaldehyde and benzene (Table 1). The generation of these carcinogenic compounds varied with the water vapor levels. Table 2 lists the concentrations of toluene and its by-products at inlet toluene concentrations of 400 ppbv and 800 ppbv (mean value and standard error with 95% confidence interval). Based on Eqs. (3)–(5), the carbon balance ratio between outlet and inlet, η_{carbon}, and the health-related index (HRI) of carcinogenic by-products (formaldehyde, acetaldehyde and benzene) were also calculated and shown in Table 2.

4. Discussion

4.1. Competitive adsorption effect

The curves shown in Fig. 2 were linked to the competitive adsorption effect between water vapor and toluene. Obee and Hay [20] applied a unimolecular Langmuir–Hinshelwood (L–H) model to analyze such a competitive adsorption effect:

$$r = k_0 \frac{KC}{1 + KC + K_W C_W} \quad (6)$$

where k_0 is the rate constant for a given UV intensity; K and K_W are the Langmuir adsorption equilibrium constants; C and C_W are the gas-phase concentrations of target pollutant and water vapor, respectively. Considering the by-products, an improved L–H model for multiple compounds was described as [25,26]:

$$r = k \frac{KC}{1 + KC + K_W C_W + \sum_i K_i C_i} \quad (7)$$

where K_i is the Langmuir adsorption equilibrium constant of by-product C_i. The generated by-products occupied the adsorption sites considered in the denominator of Eq. (7) (right side), and then resulted in the decreasing of the reaction flux. However, the types

Table 2
Concentrations of toluene and its by-products at inlet toluene concentrations of 400 ppbv and 800 ppbv.

RH (%)	Water vapor (ppmv)	Inlet (ppbv) mean ± 2 × SD (95% confidence interval)	Outlet (ppbv) mean ± 2 × SD (95% confidence interval)								ε (%)	η_{carbon} (%)	HRI_{car}
		Toluene	Toluene	Formaldehyde	Methanol	Propylene	Acetaldehyde	Acetone	Benzene	Acetic acid	Benzaldehyde			
Inlet toluene concentration of 400 ppbv														
59.4	18,840.6	421.5 ± 28.2	123.7 ± 13.3	4.8 ± 2.6	65.5 ± 8.8	8.7 ± 2.2	7.0 ± 1.8	3.4 ± 1.4	0.5 ± 0.3	6.2 ± 1.9	1.0 ± 0.9	70.7	34.2	0.8
60.9	19,322.1	392.2 ± 22.5	102.2 ± 13.6	3.6 ± 2.2	61.9 ± 9.4	5.6 ± 1.8	5.3 ± 1.7	2.9 ± 1.2	0.5 ± 0.2	6.8 ± 1.3	1.2 ± 0.6	74.0	30.7	0.6
44.8	14,169.0	394.3 ± 23.8	42.1 ± 8.9	4.2 ± 2.1	30.5 ± 6.8	3.1 ± 1.6	3.7 ± 1.5	2.5 ± 0.9	0.2 ± 0.3	3.0 ± 1.0	0.8 ± 0.6	89.3	13.3	0.7
27.2	8573.0	375.8 ± 26.9	11.9 ± 2.6	2.2 ± 1.8	5.9 ± 2.9	1.2 ± 0.8	1.5 ± 1.2	1.2 ± 0.8	0.1 ± 0.2	1.0 ± 0.7	0.2 ± 0.4	96.8	4.0	0.3
16.0	5032.0	394.3 ± 29.1	8.1 ± 2.2	1.0 ± 1.8	1.2 ± 2.0	0.9 ± 1.0	1.4 ± 1.2	1.0 ± 0.7	0.1 ± 0.2	0.4 ± 0.4	0.2 ± 0.4	98.0	2.5	0.2
3.1	972.5	404.9 ± 31.9	311.1 ± 21.2	4.1 ± 2.1	2.2 ± 2.4	0.7 ± 1.0	9.0 ± 2.9	1.7 ± 1.0	0.8 ± 0.5	0.4 ± 0.5	0.7 ± 0.7	23.2	78.3	0.7
Inlet toluene concentration of 800 ppbv														
59.3	18,808.6	808.3 ± 57.0	368.2 ± 36.1	20.2 ± 3.3	174.6 ± 18.1	2.4 ± 1.4	24.2 ± 3.0	5.0 ± 1.6	1.7 ± 0.5	0.1 ± 0.1	0.2 ± 0.3	54.5	50.5	3.3
42.1	13,308.0	810.3 ± 37.2	268.0 ± 23.0	15.1 ± 3.1	132.7 ± 13.8	1.2 ± 1.6	18.4 ± 2.2	3.3 ± 1.2	1.8 ± 0.6	4.8 ± 1.6	0.2 ± 0.4	66.9	37.0	2.5
31.2	9841.5	798.7 ± 39.5	341.9 ± 31.2	13.6 ± 2.8	92.3 ± 10.1	1.0 ± 1.1	15.2 ± 2.8	3.8 ± 1.4	1.2 ± 0.3	3.2 ± 1.7	0.5 ± 0.4	57.2	45.8	2.2
23.3	7338.3	773.2 ± 36.7	452.7 ± 33.7	5.7 ± 3.7	60.3 ± 8.7	1.7 ± 1.3	14.8 ± 3.2	4.5 ± 1.5	1.3 ± 1.2	1.5 ± 0.8	8.1 ± 2.9	41.5	61.9	1.1
10.3	3235.8	812.7 ± 41.2	631.9 ± 32.8	3.2 ± 2.5	21.3 ± 7.6	1.9 ± 1.3	13.5 ± 2.3	3.4 ± 1.3	0.3 ± 0.4	0.6 ± 0.4	0.6 ± 0.7	22.2	79.1	0.6
5.7	1789.1	815.4 ± 39.8	792.0 ± 35.7	12.4 ± 4.2	5.4 ± 2.1	2.1 ± 1.2	33.0 ± 5.4	8.9 ± 2.1	2.4 ± 0.7	1.8 ± 0.8	0.1 ± 0.2	2.9	99.5	2.3

Table 3
Unimolecular Langmuir–Hinshelwood correlation coefficients of toluene.

Coefficients	Value	Standard error (95% confidence level)
k_0 (ppbv m/s)	4.46×10^{-3}	2.11×10^{-4}
K (ppbv^{-1})	1.07	5.07×10^{-2}
K_W (ppmv^{-1})	6.29×10^{-3}	3.44×10^{-3}

of by-products and their concentrations were varied during the photocatalytic reactions (see Fig. 1). That is to say, it is difficult to estimate the exact form of the denominator in Eq. (7).

In fact, the competitive adsorption effect of by-products may make a small contribution to the reaction flux. Eq. (6) can be rewritten as:

$$\frac{1}{r} = \frac{1}{k_0} + \frac{1}{k_0 K}\frac{1}{C} + \frac{K_W}{k_0 K}\frac{C_W}{C} \quad (8)$$

The coefficients, k_0, K and K_W in Eq. (6) were obtained through multiple linear regression of the experimental data, as shown in Table 3.

As shown in Fig. 3, only a few blue dots did not agree with the linear fitting, while most of the experimental data (red dots) were in good agreement with Eq. (8), R^2 equal to 0.9565. This indicated that in general the term $\sum_i K_i C_i$ has a negligible effect on the denominator in Eq. (7), that is, no significant competitive adsorption effect of by-products occurs. In such a situation, the complicated Eq. (7) can be replaced with the simple model as Eq. (6) to estimate the PCO reaction flux.

However, the term $\sum_i K_i C_i$ cannot be neglected at low water vapor levels. The outliers (blue dots in Fig. 3) were all obtained at low relative humidities (<16%, see Table S1), probably due to the deactivation caused by the accumulation of by-products on the reaction surface [27]. This problem will be exacerbated in real indoor applications involving numerous simultaneous pollutants (reactants) that will be accompanied by more potential by-products. Obviously, it may be impossible to determine or predict how many by-products are generated during a practical PCO process. Although there have been many studies to obtain the adsorption equilibrium constants, K in laboratories [28,29], it has to be acknowledged that the obtained K may only be used when no deactivation occurs or when only a few by-products are generated, probably with a high water vapor concentration.

Supplementary material related to this article found, in the online version, at http://dx.doi.org/10.1016/j.apcatb.2012.12.001.

4.2. Maximum efficiency does not always lead to minimal by-products

Fig. 4 shows the decomposition efficiencies and the concentrations of three main carcinogenic by-products (formaldehyde, acetaldehyde and benzene) at the outlet of the photocatalytic reactor. In the case of an initial toluene concentration of 400 ppbv, the higher the efficiency was, the lower the concentrations of carcinogenic by-products were. However, when the initial toluene concentration was 800 ppbv, the maximum efficiency and minimum concentrations of carcinogenic by-products were obtained at the relative humidity of 42.1% and 10.3%, respectively, showing that maximum efficiency does not always lead to minimal by-products.

Water vapor has both active and inhibiting effects on the photocatalytic oxidation process. It has been already improved that the photogenerated positive holes will drive the oxidation of compounds adsorbed on the surface of a photocatalyst [30]. But the holes will react with adsorbed water and generate hydroxyl radical (OH•), which is the dominant strong oxidant [31]. Therefore, water plays a key positive role on PCO reaction. However, another function of water is the competitive adsorption effect with other

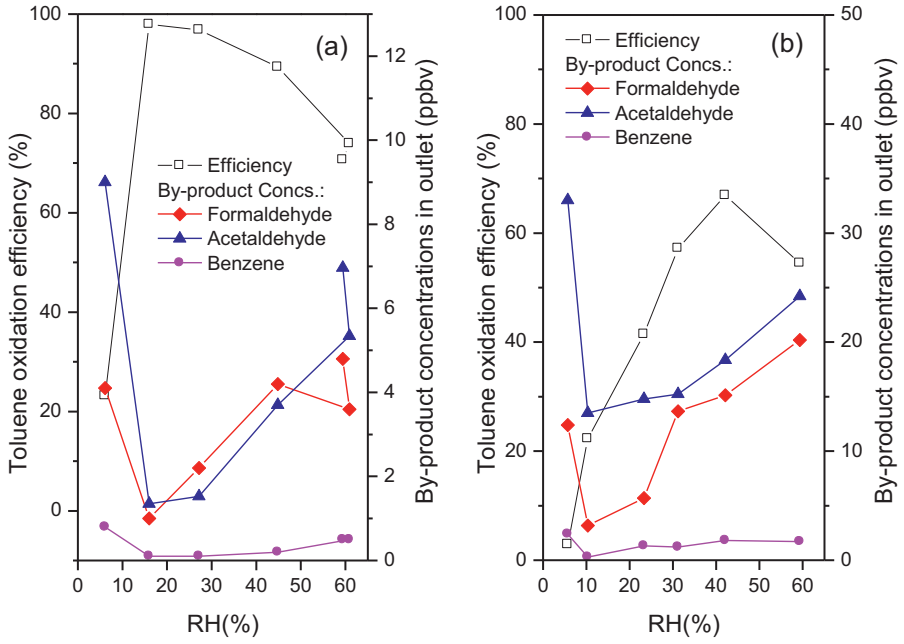

Fig. 4. Toluene oxidation efficiency and by-product concentrations versus relative humidity with inlet toluene concentrations of (a) 400 ppbv and (b) 800 ppbv.

compounds [31,32]. Fig. 5 shows the possible effect of water vapor on the by-product production. When the concentration of water vapor is extremely high, competitive adsorption with water reduces the residence time of the by-products on the surface of the photocatalyst. Both low and high molecular weight by-products quickly release from the surface and are detected in the gas phase (Fig. 5(a)).

When the concentration of water vapor is decreasing, this competitive adsorption is inhibited. More and more toluene and its by-products are adsorbed on the photocatalytic surface, resulting in the higher toluene decomposed efficiency and lower generation of by-products (Fig. 5(b)). There is a balance between the active and inhibiting effects of water. If the formation of HO• radicals is exactly consumed by adsorbed toluene and its by-products, a minimal quantity of by-products is obtained. If the OH• only matches the demand of toluene decomposition but not its by-products simultaneously. A maximum efficiency of toluene removal is obtained. Meanwhile, more by-products will release into gas phase due to the lack of HO• radicals. Thus, the maximum efficiency and minimal by-product generation do not occur at the same water vapor concentration (see Fig. 4(b)). It should be pointed out that this phenomenon seems to happen at high toluene concentration. When the concentration of toluene is 400 ppbv, the maximum efficiency and minimum concentrations of carcinogenic by-products were obtained at the same relative humidity of 16.0% (Fig. 4(a)).

When the water vapor level approaches 0 (Fig. 5(c)), the by-products accumulated on the reaction surface and blocked the photocatalyst [13,15] resulting in a deactivation of the photocatalyst (Fig. 1(b)). In our study, acetaldehyde was the main by-product at low water vapor levels. This is consistent with the results of

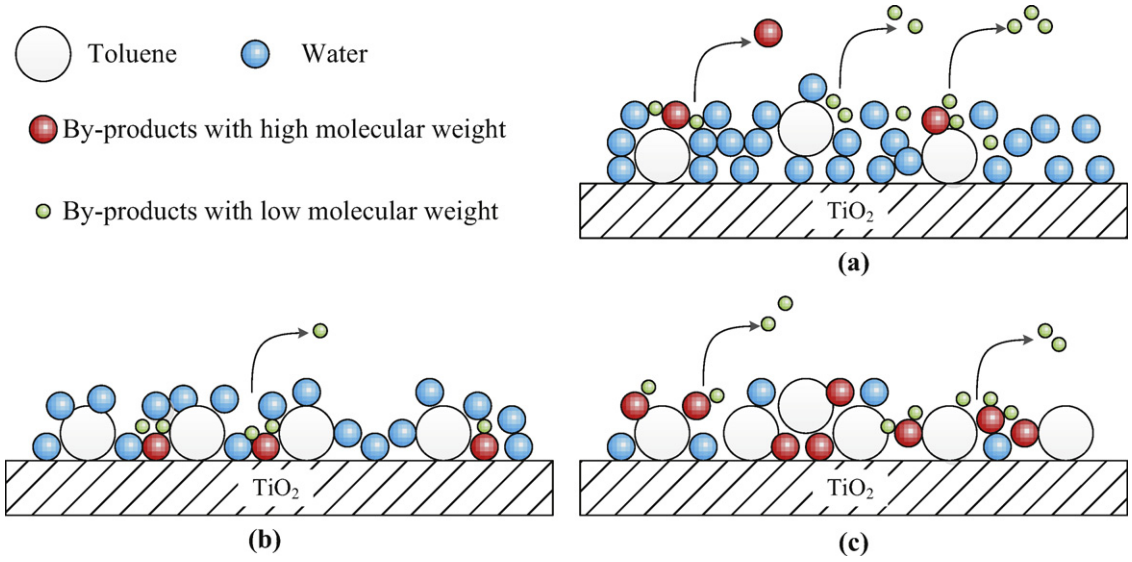

Fig. 5. Effect of water vapor on the by-product production.

Sleiman et al. [15] who found that some small aldehydes were produced in the gas phase at low water vapor concentration. In addition, we found many high molecular weight by-products adsorbed on the surface in our previous study [13]. However, Sleiman et al. [15] found there were fewer high molecular weight by-products, such as benzaldehyde at low water vapor concentration, compared with that at high water vapor concentration after 1 or 3 days reaction time. The reason may be that the photocatalyst deactivates very early at low water vapor concentration and does not generate any by-products later, thus the high molecular weight by-products adsorbed on the surface or in gas phase were finally less than that found with high water vapor concentrations.

The removal efficiency of an air cleaner is commonly used to assess whether the purification performance is good or bad [33]. However, Table 2 shows that the inconsistency between maximum efficiency and minimal by-product generation also resulted in different health risk (HRI_{car}) values of the PCO purification at different water vapor concentrations. Therefore, we need to take the health risk (such as the HRI value) as the optimized target and not the maximum decomposition efficiency when evaluating the performance of photocatalytic air purification.

5. Conclusions

Water vapor has a significant effect not only on the photocatalytic decomposition rate of toluene, but also its by-products generations. It is due to the competitive adsorption among water vapor, toluene and its by-products. High water vapor concentrations reduce the residence time of the by-products on the reaction surface and hasten their release from the surface. Lower water vapor concentrations normally result in higher decomposition efficiency and lower by-product generation. But the extremely low water vapor concentrations lead to the deactivation of photocatalyst. The diversity of by-products during a photocatalytic reaction may make the common-used Langmuir–Hinshelwood model unfeasible in real practical application. Maximum decomposition efficiency does not always lead to minimal by-products and lowest healthy risk. Health risks posed by the by-products should be the primary concern rather than the decomposition efficiency when evaluating the performance of photocatalytic air purification.

Acknowledgements

The authors thank Prof. Yadong Li, Dept. of Chemistry, Tsinghua University for valuable discussions. This study was supported by National Nature Science Foundation of China (51136002, 51006057) and the 12th Five-years National Key Technology R&D Program (2012BAJ02B-03 and 2012BAJ02B-07).

References

[1] J.C. Little, A.T. Hodgson, A.J. Gadgil, Atmospheric Environment 28 (1994) 227–234.
[2] Y. Xu, Y.P. Zhang, Atmospheric Environment 37 (2003) 2497–2505.
[3] L.Z. Zhang, J.L. Niu, Building and Environment 39 (2004) 523–531.
[4] C. Kwong, C.Y.H. Chao, K.S. Hui, M.P. Wan, Atmospheric Environment 42 (2008) 2300–2311.
[5] M.J. Finnegan, C.A.C. Pickering, P.S. Burge, British Medical Journal 289 (1984) 1573–1575.
[6] D.K. Sari, S. Kuwahara, Y. Tsukamoto, H. Hori, N. Kunugita, K. Arashidani, H. Fujimaki, F. Sasaki, Brain Research 1013 (2004) 107–116.
[7] Y.P. Zhang, R. Yang, R.Y. Zhao, Atmospheric Environment 37 (2003) 3395–3399.
[8] D.T. Tompkins, B.J. Lawnicki, W.A. Zeltner, M.A. Anderson, ASHRAE Transactions 111 (2005) 60–84.
[9] X.M. Sun, Y.D. Li, Chemistry – A European Journal 9 (2003) 2229–2238.
[10] Z.B. Wu, F. Dong, W.R. Zhao, S. Guo, Journal of Hazardous Materials 157 (2008) 57–63.
[11] Y.P. Zhang, J.H. Mo, Y.G. Li, J. Sundell, P. Wargocki, J.S. Zhang, J.C. Little, R. Corsi, Q.H. Deng, M.H.K. Leung, L. Fang, W.H. Chen, J.G. Li, Y.X. Sun, Atmospheric Environment 45 (2011) 4329–4343.
[12] V. Augugliaro, S. Coluccia, V. Loddo, L. Marchese, G. Martra, L. Palmisano, M. Schiavello, Applied Catalysis B 20 (1999) 15–27.
[13] J.H. Mo, Y.P. Zhang, Q.J. Xu, Y.F. Zhu, J.J. Lamson, R.Y. Zhao, Applied Catalysis B 89 (2009) 570–576.
[14] S.O. Hay, T.N. Obee, C. Thibaud-Erkey, Applied Catalysis B 99 (2010) 435–441.
[15] M. Sleiman, P. Conchon, C. Ferronato, J.M. Chovelon, Applied Catalysis B 86 (2009) 159–165.
[16] A. Wisthaler, P. Strøm-Tejsen, L. Fang, T.J. Arnaud, A. Hansel, T.D. Märk, D.P. Wyon, Environmental Science and Technology 41 (2007) 229–234.
[17] J.H. Mo, Y.P. Zhang, R. Yang, Indoor Air 15 (2005) 291–300.
[18] L.F. Zhang, W.A. Anderson, S. Sawell, C. Moralejo, Chemosphere 68 (2007) 546–553.
[19] X.Z. Fu, L.A. Clark, W.A. Zeltner, M.A. Anderson, Journal of Photochemistry and Photobiology A 97 (1996) 181–186.
[20] T.N. Obee, S.O. Hay, Environmental Science and Technology 31 (1997) 2034–2038.
[21] Y. Ku, K.Y. Tseng, W.Y. Wang, Water, Air, & Soil Pollution 168 (2005) 313–323.
[22] M. Sleiman, C. Ferronato, J.M. Chovelon, Environmental Science and Technology 42 (2008) 3018–3024.
[23] O. d'Hennezel, P. Pichat, D.F. Ollis, Journal of Photochemistry and Photobiology A 118 (1998) 197–204.
[24] A. Wisthaler, C.J. Weschler, Proceedings of the National Academy of Sciences of the United States of America 107 (2010) 6568–6575.
[25] W. Chen, J.S. Zhang, Building and Environment 43 (2008) 246–252.
[26] G. Vincent, P.M. Marquaire, O. Zahraa, Journal of Hazardous Materials 161 (2009) 1173–1181.
[27] M. Addamo, V. Augugliaro, S. Coluccia, A. Di Paola, E. Garcia-Lopez, V. Loddo, G. Marci, G. Martra, L. Palmisano, International Journal of Photoenergy (2006) 1–12, Article ID 39182.
[28] A. Bouzaza, C. Vallet, A. Laplanche, Journal of Photochemistry and Photobiology A 177 (2006) 212–217.
[29] J.B. Zhong, J.L. Wang, L. Tao, M.C. Gong, Z.L. Liu, Y.Q. Chen, Journal of Hazardous Materials 139 (2007) 323–331.
[30] B. Ohtani, Chemistry Letters 37 (2008) 217–229.
[31] H. Einaga, S. Futamura, T. Ibusuki, Applied Catalysis B 38 (2002) 215–225.
[32] C. Raillard, V. Hequet, P. Le Cloirec, J. Legrand, Journal of Photochemistry and Photobiology A 163 (2004) 425–431.
[33] ANSI/AHAM Standard AC-1, Association of Home Appliance Manufacturers (2005).